Mathematical Modeling of Encapsulated Buffer Performance in Sand Columns

Lubo Liu[1]; Christine M. Rust[2]; Joseph R. V. Flora[3]; and C. Marjorie Aelion[4]

Abstract: A one-dimensional mathematical model was developed to simulate pH control using an encapsulated phosphate buffer during denitrification in a sand column. The parameters required for the model were obtained from direct physical measurement, from a tracer study to characterize the dispersion coefficient in the column, and from batch experiments designed to obtain an empirical expression describing the variation of the first-order rate constant for the encapsulated buffer core release with pH. First-order kinetic constants describing the rates of denitrification and ethanol biodegradation were obtained by fitting the model to column runs without the encapsulated buffer. With these parameters, the model was subsequently used to predict the performance of column runs containing the encapsulated buffer. Since denitrification was essentially complete in the sand columns, an increase in the effluent pH was observed. This pH increase was counteracted by the controlled release of the acidic core of the encapsulated buffers added in the columns. The model reasonably predicted the release of the encapsulated buffer core and the performance of the encapsulated buffer for controlling pH in the column.

DOI: 10.1061/(ASCE)0733-9372(2002)128:12(1128)

CE Database keywords: Mathematical models; Denitrification; Columns; Sand.

Introduction

Maintenance of a process in an optimum pH range can be a prerequisite to the effectiveness of numerous chemical and biological processes in environmental engineering. For example, it has been shown that the effectiveness of bioremediation is impacted by pH (Goodwin et al. 1988; Reardon and Bailey 1989; Albrechtsen 1994). It has also been shown that the rate of reduction of halogenated compounds by zero-valent metals is faster at a lower pH (Matheson and Tratnyek 1994). Controlling the pH in an in situ remediation scenario by pumping acids or bases through wells or infiltration galleries may be technically difficult and capital intensive. A promising method of effectively controlling the pH in an in situ remediation scenario is through the use of encapsulated buffers. Vanukuru et al. (1998) used encapsulated buffers comprised of an acidic phosphate core and a pH sensitive polymer wall that dissolves in solutions with a pH greater than 7.0. The wall dissolves faster at a higher pH, hence releasing more of the acidic core contents to reduce the pH of the surrounding solution. The encapsulated buffer can potentially be delivered through injection wells and left in the well without the need for additional equipment.

Rust et al. (2002) demonstrated that the encapsulated buffers are effective in controlling the pH in sand columns with an active denitrifying population. During denitrification, the reduction of nitrate to nitrogen gas increases the effluent pH from the column. After the injection of encapsulated buffers in the column, the high pH dissolves the polymer wall and releases the phosphate buffer to decrease the pH. In this study, a mathematical model for the sand column is developed to understand the pH control mechanisms that occur in the column.

Numerous one-dimensional advection–dispersion models simulating chemical equilibrium, chemical reactions, and the transport and fate of chemical species have been reported in the literature (Furrer et al. 1996; Bäverman et al. 1999; von Gunten and Furrer 2000). Some models have also accounted for the pH changes in a system (Appelo 1994; Haran et al. 1997; Choi et al. 1998). Some commercial and public domain models are available that calculate geochemical speciation and are commonly based on the assumption that local chemical equilibrium and thermodynamically well-defined mineral phases exist at every point. Examples of such programs include: *MICROQL* (Swiss Federal Institute of Technology, Duebendorf, Switzerland 1979); *EQ6*: (Wolery and Daveler 1992); *PHREEQE* (Parkhurst 1995); and *MINTEQA2* (Allison et al. 1991). The typical drawback to adapting these models to a specific case is that the learning curve can be steep and altering the model to be applicable to one's system is difficult. Thus, the approach taken in this study was to develop a one-dimensional model that was specifically applicable for the experimental sand column.

The specific objective of this study is to develop a one-dimensional mathematical model to simulate pH control using an encapsulated phosphate buffer during denitrification in a sand column. The model accounts for advection and dispersion, acid-base equilibrium, electroneutrality, biological reactions, and the kinet-

[1]Dept. of Civil and Environmental Engineering, Univ. of South Carolina, 300 Main St., Columbia, SC 29208.

[2]Dept. of Environmental Health Sciences, School of Public Health, Univ. of South Carolina, Columbia, SC 29208.

[3]Dept. of Civil and Environmental Engineering, Univ. of South Carolina, 300 Main St., Columbia, SC 29208 (corresponding author). E-mail: flora-joseph@sc.edu

[4]Dept. of Environmental Health Sciences, School of Public Health, Univ. of South Carolina, Columbia, SC 29208.

Note. Associate Editor: George A. Sorial. Discussion open until May 1, 2003. Separate discussions must be submitted for individual papers. To extend the closing date by one month, a written request must be filed with the ASCE Managing Editor. The manuscript for this paper was submitted for review and possible publication on August 24, 2001; approved on March 19, 2002. This paper is part of the ***Journal of Environmental Engineering***, Vol. 128, No. 12, December 1, 2002. ©ASCE, ISSN 0733-9372/2002/12-1128–1138/$8.00+$.50 per page.

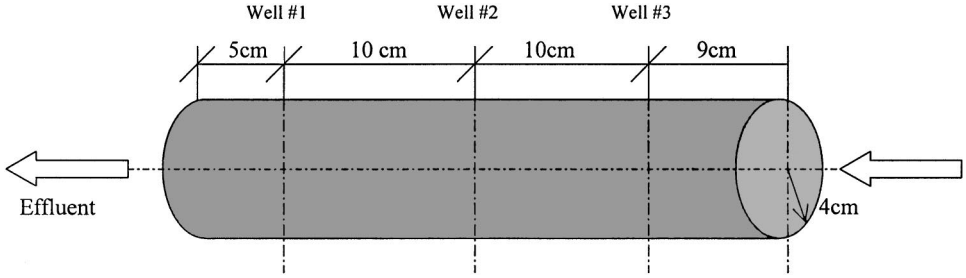

Fig. 1. Schematic of flow-through sand column showing location of wells containing encapsulated buffer

ics of release of the encapsulated buffer core. The parameters required for the model were obtained from previous experiments, and the model predictions of the performance of the encapsulated buffer in controlling the pH in the column were evaluated. The modeling approach could potentially be extended to two or three dimensions and used in remediation applications where pH control is desirable.
speciation,

Materials and Methods

The experiments in the succeeding paragraphs are described in detail in Vanukuru et al. (1998); Rust (2001); and Rust et al. (2002). For completeness, a brief description of the previous work is outlined.

Characterization of Encapsulated Buffer

The encapsulated buffer used in this study is in microcapsule form (≈0.5–2 mm in diameter) composed of an acidic phosphate core (KH_2PO_4) coated with a methacrylic acid copolymer (Eudragit™ S-100, Rohm America Inc., Piscataway, N.J.). The mass ratio between the phosphate core and the polymer coating is 7:3. At a solution pH greater than 7.0, the polymer dissolves and releases the acidic core. The release of the core contents of the encapsulated buffer was characterized in batch studies at different constant pH values ranging from 6 to 9. Previously, a model was developed that described the kinetics of release of the buffer core using Monte Carlo methods (Vanukuru et al. 1998). However, incorporating this stochastic approach into a model for a sand column is computationally intensive. Thus, a deterministic model was developed to fit the experimental data and obtain a new set of kinetic parameters.

Sand Column Experiments

Fig. 1 shows a schematic of the glass column used to test the capacity of the encapsulated buffer in controlling pH in a flow-through scenario. Denitrification occurred in the column using ethanol as the electron donor and carbon source. Three miniature wells were installed at different points along the column to hold the encapsulated buffer, and equal masses of encapsulated buffer were added to each of these three wells. The column was fed by timed peristaltic pumps, which provided intermittent flow from one feed reservoir at a cycle of 6 s on and 54 s off. The pH and concentration of the ethanol [reported as total organic carbon during the first column run and subsequently as ethanol during the second column run], phosphate, nitrate–nitrogen, and total inorganic carbon in both the influent and effluent were monitored.

In the first and second column runs, a biologically active column without encapsulated buffer, a biologically active column with encapsulated buffer, and an abiotic column were operated. The major difference between column runs is that trichloroethylene (TCE) was added in the second column run to evaluate simultaneous denitrification and degradation of TCE within the column, and that the influent phosphate levels in the second column run were decreased significantly. The TCE measured in the column influent ranged from 0.2 to 1.5 mg/L in the experiments due to the volatile nature of TCE. Denitrification was not observed in the abiotic control column. Models were developed for the biologically active columns in the study. In this manuscript, Columns A and B refer to the columns without and with encapsulated buffer addition, respectively. Cases I and II refer to the first column run without the addition of TCE and the second column run with the addition of TCE, respectively. For Column B, 5 and 3 g of encapsulated buffer were added in each well for Cases I and II, respectively. Table 1 shows a summary of the experimental matrix of column runs.

Mathematical Model

A one-dimensional mathematical model was developed to simulate the biological and chemical processes occurring in the column. Neglecting biomass growth and decay, the stoichiometry of denitrification can be written as

$$5CH_3CH_2OH + 12H^+ + 12NO_3^- \rightarrow 10CO_2 + 6N_2 + 21H_2O \quad (1)$$

Since an excess of ethanol was added to the column, and the amount of decrease of ethanol could not be attributed to pure denitrification alone, another reaction was simulated to account for the missing ethanol. The most suitable reaction in the absence of other electron acceptors is a fermentation type reaction

Table 1. Summary of Experimental Runs

	Column A	Column B
Case I	Without capsules Without TCE	With capsules Without TCE
Case II	Without capsules With TCE	With capsules With TCE

$$CH_3CH_2OH \rightarrow 1.5CH_4 + 0.5CO_2 \quad (2)$$

The reduction of nitrate to nitrogen gas results in an increase in the pH of the column. Although the production of CO_2 from Eq. (2) may cause a decrease in the pH, the effect of Eq. (1) on the pH dominates the system.

The overall change in pH depends on the buffer capacity of the system. Because the sand used in this study had negligible buffer capacity, the chemical equilibrium of the solution determines the overall change in pH. The following expressions describing nitrate, phosphate, and carbonate equilibrium and water dissociation were used in the model:

$$K_{NO_3,1} = \frac{[H^+][NO_3^-]}{[HNO_3]} = 10^0 \quad (3)$$

$$K_{CO_3,1} = \frac{[H^+][HCO_3^-]}{[H_2CO_3^*]} = 10^{-6.3} \quad (4)$$

$$K_{CO_3,2} = \frac{[H^+][CO_3^{2-}]}{[HCO_3^-]} = 10^{-10.3} \quad (5)$$

$$K_{PO_4,1} = \frac{[H^+][H_2PO_4^-]}{[H_3PO_4]} = 10^{-2.1} \quad (6)$$

$$K_{PO_4,2} = \frac{[H^+][HPO_4^{2-}]}{[H_2PO_4^-]} = 10^{-7.2} \quad (7)$$

$$K_{PO_4,3} = \frac{[H^+][PO_4^{3-}]}{[HPO_4^{2-}]} = 10^{-12.3} \quad (8)$$

$$K_w = [H^+][OH^-] = 10^{-14} \quad (9)$$

where $K_{i,j} = j$th dissociation constant of the ith species; and K_w = equilibrium constant of water dissociation. Values for the dissociation constants were obtained from Snoeyink and Jenkins (1980). Because the model for the system accounts for pH changes and involves ionic species, the net sum of all cationic and anionic charges at every point in the system is zero. The formation of complexes in solution can be neglected because of the trace amounts of metal cations in the system. Thus, the electroneutrality condition can be expressed as

$$[H^+] + [K^+] = [OH^-] + [HCO_3^-] + 2[CO_3^{2-}] + [H_2PO_4^-] + 2[HPO_4^{2-}] + 3[PO_4^{3-}] + [NO_3^-] \quad (10)$$

Transport of the various species j through the column was described as follows:

$$\frac{\partial C_j}{\partial t} + u\frac{\partial C_j}{\partial x} = D\frac{\partial^2 C_j}{\partial x^2} + R_j \quad (11)$$

where C_j = concentration of the jth species (M/L^3); u = linear water velocity through the column (L/T); x = axial distance along the column (L); D = dispersion coefficient (L^2/T); and R_j = rate of production of species j (M/L^{3}T). The subscript j represents the following chemical species: K^+, CH_3CH_2OH, total nitrate species ($[HNO_3]+[NO_3^-]$), total phosphate species ($[H_3PO_4]+[H_2PO_4^-]+[HPO_4^{2-}]+[PO_4^{3-}]$), and total carbonate species ($[H_2CO_3^*]+[HCO_3^-]+[CO_3^{2-}]$). A mass balance on TCE was not included in the model because the degradation of TCE was not detected during the second column run (Case II).

The following expression is used to describe the rate of encapsulated buffer core release in the wells:

$$\frac{dC_{K^+}}{dt} = R_{K^+} \quad (12)$$

$$\frac{dC_{T,PO_4}}{dt} = R_{C_{T,PO_4}} = \frac{MW_{H_2PO_4^-}}{MW_{K^+}} R_{K^+} \quad (13)$$

Because the encapsulated buffer was added in stationary wells and did not move as the water flowed through the wells, Eqs. (12) and (13) are only valid at each well location.

In-depth biological studies (e.g., microcosm studies) to determine the rates of the microbially-mediated reactions [Eqs. (1) and (2)] were not performed. Thus, Eqs. (1) and (2) were assumed to be nitrate limited and ethanol limited, respectively, with their degradation rate defined by the following bulk first-order kinetic expressions:

$$R_{NO_3} = -k_{NO_3}C_{NO_3} \quad (14)$$

$$R_{CH_3CH_2OH,2} = -k_{CH_3CH_2OH}C_{CH_3CH_2OH} \quad (15)$$

where k_{NO_3} and $k_{CH_3CH_2OH}$ = first order reaction rate coefficients of nitrate and ethanol, respectively ($1/T$). Bulk kinetic expressions were used instead of a biofilm model to simplify the modeling approach. Spatial variations of the micro-organism population that mediate the two reactions could occur as a result of differing redox conditions along the column. These variations are neglected because most of the modeling results focus on the column effluent quality. From Eqs. (1) and (2), the overall rate of ethanol degradation and total carbonate production (from carbon dioxide production) can be written as

$$R_{CH_3CH_2OH} = R_{CH_3CH_2OH,1} + R_{CH_3CH_2OH,2} = -\frac{5}{12}\frac{MW_{CH_3CH_2OH}}{MW_{NO_3}}k_{NO_3}C_{NO_3} - k_{CH_3CH_2OH}C_{CH_3CH_2OH} \quad (16)$$

$$R_{CO_3} = \frac{10}{12}\frac{MW_{CO_2}}{MW_{NO_3}}k_{NO_3}C_{NO_3} + 0.5k_{CH_3CH_2OH}C_{CH_3CH_2OH} \quad (17)$$

Eqs. (3)–(14), (16), and (17) represent the overall mathematical model for the sand column. The control volume method was used to solve the system of equations where the space domain was divided into 340 nonoverlapping uniform control volumes. The equations were integrated over each control volume at each time step and piecewise profiles expressing the concentration variation between the control volumes were used to evaluate the required integrals (Patankar 1980). An implicit time stepping scheme with a time step of 100 s was used to integrate the system of equations over time. Iterative procedures were performed because various terms in the system of equations are interdependent (e.g., pH). The initial and boundary conditions necessary to solve the model are

$$C_j = C_{j0} \quad \text{at } t = 0 \quad (18)$$

$$C_j = C_{j,inf} \quad \text{at } x = 0 \quad (19)$$

$$\frac{dC_j}{dx} = 0 \quad \text{at } x = L \quad (20)$$

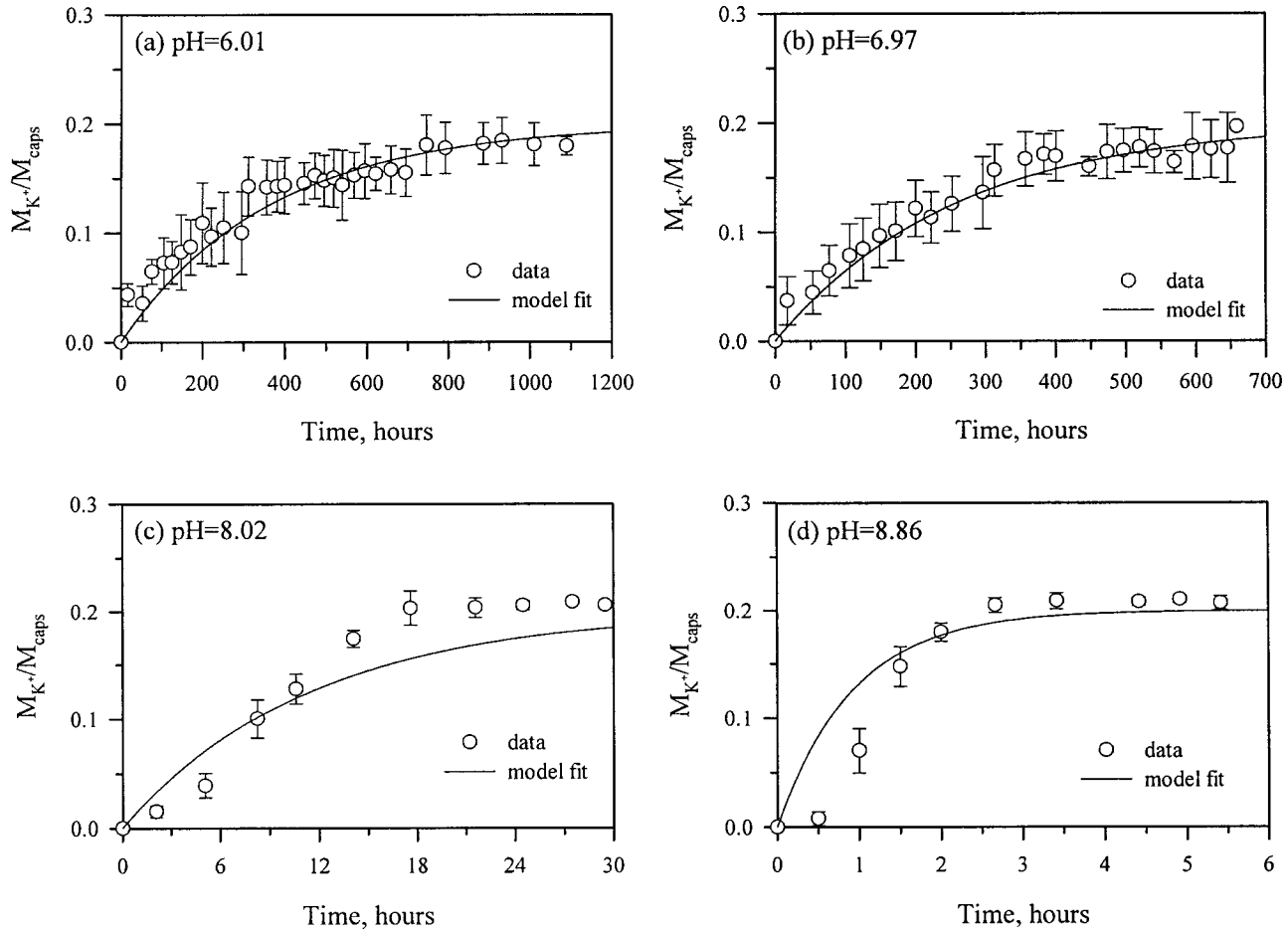

Fig. 2. Representative experiments showing encapsulated buffer core release at various pH values (Vanukuru 1998), data were fit with first-order kinetic constant [see Eq. (21)]

where C_{j0} = initial concentration of the jth species; and $C_{j,\text{inf}}$ = concentration of the jth species in the column influent. The initial conditions were taken to be the conditions in the column after 4 and 6 days for Cases I and II, respectively. These days represent the time when microcapsules were added in the wells of Column B. The influent conditions to the column during times where data were unavailable were obtained through parabolic interpolation from the available data. The algorithm produces mass balance errors that are less than 1%.

Results and Discussion

The rate of release of the encapsulated buffer core was assumed to follow first-order kinetics,

$$\frac{dM_c}{dt} = -\alpha M_c \tag{21}$$

where M_c = mass of the KH_2PO_4 core; and α = first order kinetic constant. Fig. 2 shows the mass of potassium released (normalized to the total mass of potassium) for various pH levels and the first-order kinetic model fit. Overall, the model fit the data quite well at low pH values where the primary core release mechanism is diffusion through the encapsulated buffer wall. At higher values, where the primary release mechanism is wall erosion and core dissolution, the model fit is not as good compared to the lower pH. Future studies should evaluate the accuracy of the model predictions using a stochastic approach. Knowing α, Eq. (12) can be rewritten as

$$R_{K^+} = \alpha \frac{M_c \cdot \text{MW}_K}{\text{MW}_{KH_2PO_4} \cdot V_{\text{well}} \varepsilon} \tag{22}$$

where V_{well} = volume of the well (L^3); and ε = porosity of the sand column (−).

Fig. 3 shows the variation of the first-order kinetic constant as a function of pH. The pα values decrease at higher pH values (or α increases with pH), and this relationship can be described by

$$p\alpha = -\log \alpha = -0.25 + \frac{2.83}{1 + \exp\left(\frac{\text{pH} - 7.97}{0.36}\right)} \tag{23}$$

At high pH values, the encapsulated buffer will release more mass of the phosphate core to attempt to bring the pH of the system down. As the pH decreases in the system, the rate at which the phosphate core is released will also be lowered. Thus, the encapsulated buffer serves as a proportional pH controller where the rate of acid release is self adjusting.

Tracer tests were performed to characterize the hydrodynamics in the columns. 10 mL of a blue dye was injected into the columns over a period of 17 min, and the absorbance of the dye in the effluent was monitored. Fig. 4 shows the residence time dis-

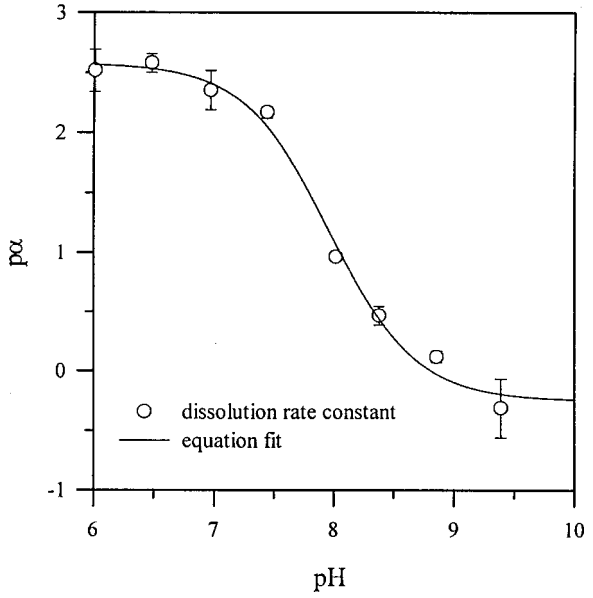

Fig. 3. Variation of dissolution rate kinetic constant [expressed as $-\log(\alpha)$] with pH

tribution function E_t and the data fit using a plug flow model with dispersion. The dispersion numbers were 1.7×10^{-2} and 6.4×10^{-3} for Columns A and B, respectively, both indicating a small deviation from plug flow (Levenspeil 1993). Using physical parameters directly measured from the experiments (i.e., flowrate, column length, porosity, and cross-sectional area), the dispersion coefficients were calculated to be 2.2×10^{-8} and 8.0×10^{-9} m^2/s in Columns A and B, respectively. Although care was taken to ensure packing of the column material would be similar, differences in dispersion coefficient could be due to slight differences in packing between columns. Table 2 shows a summary of the physical parameters used in the model.

Table 2. Physical Parameters Used in This Model

Physical parameters	Column A	Column B
Length of Column L (cm)	34	34
Flow Rate Q (mL/min)	0.48	0.42
Column inner radius R (cm)	4.0	4.0
Detention time τ (h)	24.4	25.6
Dispersion coefficient D (m^2/s)	2.2×10^{-8}	8.0×10^{-9}
Porosity of sand ε (−)	0.41	0.38
Linear velocity u (m/s)	3.9×10^{-6}	3.7×10^{-6}

To estimate the biokinetic parameters k_{NO_3} and $k_{CH_3CH_2OH}$ for each column run, the model was fit to the pH and ethanol data for the columns without the encapsulated buffer (i.e., Column A). pH was selected rather than nitrate as the fitting parameter because the nitrate levels in the column effluent were close to zero and the rise in pH is related to the extent of denitrification in the system. The sum of the squares of the differences between the model output and the data [i.e., sum of squares of errors (SSE)] was minimized by varying k_{NO_3} between 10^{-6} and 10^{-2} s^{-1} and $k_{CH_3CH_2OH}$ between 10^{-6} and 10^{-3} s^{-1}. The approach taken in this study was to obtain two sets of kinetic parameters from the ethanol and pH data of Column A for Cases I and II. The SSE for each case was calculated by normalizing to the average data as follows:

$$\text{SSE}=\sum\left[\left(\frac{C_{CH_3CH_2OH,\text{model}}-C_{CH_3CH_2OH,\text{data}}}{\overline{C}_{CH_3CH_2OH,\text{data}}}\right)^2+\left(\frac{\text{pH}_{\text{model}}-\text{pH}_{\text{data}}}{\overline{\text{pH}_{\text{data}}}}\right)^2\right] \quad (24)$$

where $C_{CH_3CH_2OH,\text{model}}$, $C_{CH_3CH_2OH,\text{data}}$, and $\overline{C}_{CH_3CH_2OH,\text{data}}$ = model output, experimental data, and average concentration,

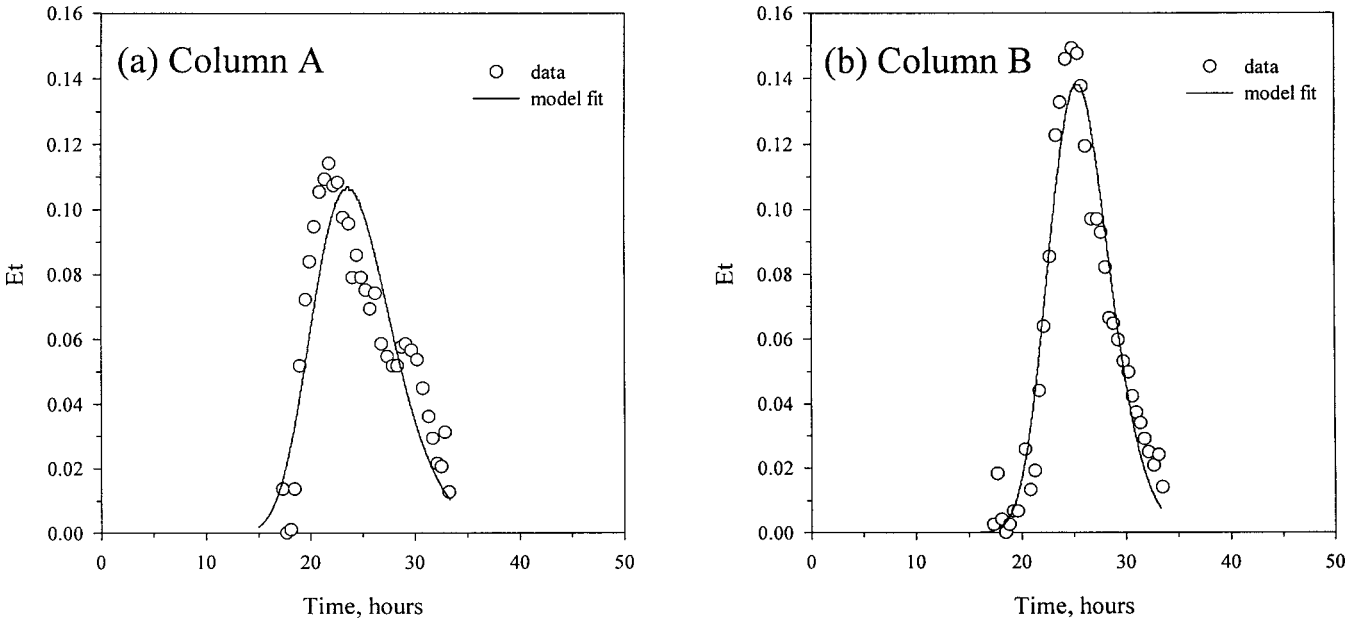

Fig. 4. Tracer fit of (a) biologically active column without encapsulated buffer (Column A), and (b) biologically active column with encapsulated buffer (Column B)

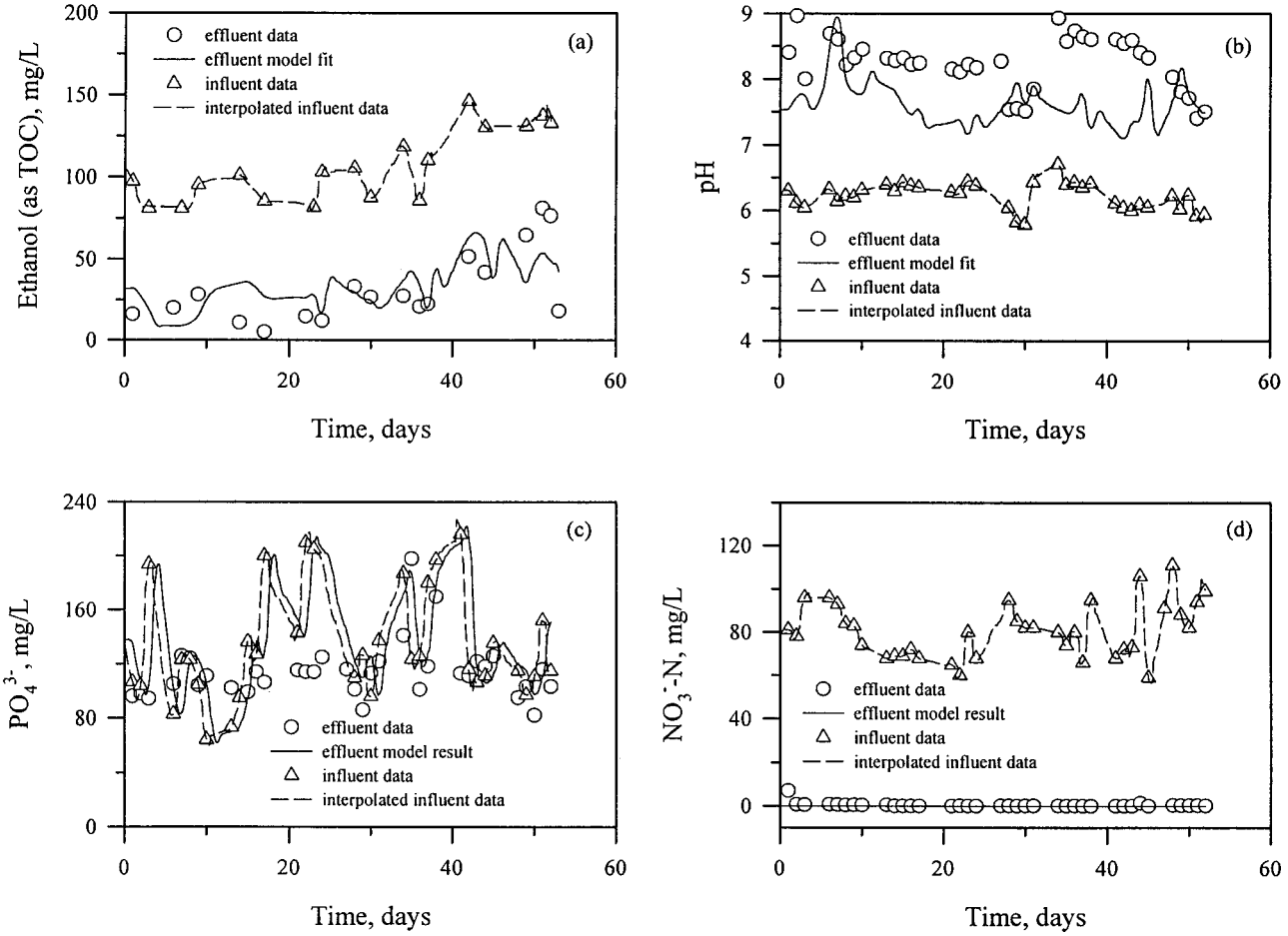

Fig. 5. Experimental data and model fit for (a) ethanol and (b) pH, and experimental data and model results for (c) phosphate and (d) nitrate for biologically active column without addition of encapsulated buffers and trichloroethylene (Column A, Case I)

respectively, of ethanol in the column effluent; and pH_{model}, pH_{data}, and $\overline{pH}_{data}$ = model output, experimental data, and average experimental data, respectively, of the effluent column pH. Normalizing to the average value scaled the magnitude of the errors such that the differences in pH and ethanol are comparable. Using these kinetic parameters, the performance of Column B for Cases I and II was predicted.

Figs. 5 and 6 show the experimental data for Column A for Cases I and II, respectively. In both cases, a decrease in ethanol concentration was detected in the effluent of the column, with an ethanol removal efficiency (based on the average of the influent and effluent) of 69 and 52% for Cases I and II, respectively. With the exception of a few data points, the nitrate concentration in the effluent was always less than 1 mg/L, indicating essentially complete denitrification within the column. The average nitrate removal efficiency (based on the average of the influent and effluent) in the column was 99.5 and 99.1% for Cases I and II, respectively. This indicates that denitrification was not impacted by the presence of TCE in the column influent. The denitrification within the column resulted in a 2.0 and 1.0 pH unit increase in the effluent. There was a lower rise in the pH for Case II because of the overall lower values of influent nitrate into the column.

Since Column A did not have any encapsulated buffer added to the column, the phosphate concentration in the effluent should be equal to the influent levels. There was less variability in the effluent phosphate levels in Case I compared to the influent levels, particularly in the first half of the column run. An analysis of variance (Neter et al. 1990) test shows that the phosphate levels in the influent (133 ± 41) are significantly higher than the effluent (114 ± 21 mg/L) ($p = 0.017$). It is possible that the decrease in variability and levels may be caused by interactions (e.g., ion exchange) between the phosphate in solution and the constituents in the column (e.g., biomass) or precipitation caused by the higher pH in column.

The model fit to the data is also shown in Figs. 5 and 6. For both Case I and II, the values for k_{NO_3} and $k_{CH_3CH_2OH}$ were 3×10^{-4} and 5×10^{-6} s^{-1}, respectively. Thus, the presence of 0.2–1.5 mg/L of TCE in Case II did not affect the denitrification and ethanol degradation rates. The model was able to reasonably fit the ethanol data. When fitting the model to the pH and ethanol data, the model results are consistent with the low effluent nitrate levels (<1 mg/L) observed during the study. Because phosphate was modeled without any reactions and the tracer study showed that the column behaved very close to a plug-flow reactor, the model shows that effluent phosphate should be almost a mirror of the influent phosphate but with a time delay equal to the detention time in the column. However, as discussed earlier, interactions between the phosphate and the column constituents may have caused this discrepancy.

Although the model generally followed the same pH trends as the experiment where the effluent levels are higher than the influent, the model fit to the pH data was fair. In Case I, the fit was generally lower than the data. Although increasing the extent of denitrification (hence increasing k_{NO_3}) could theoretically in-

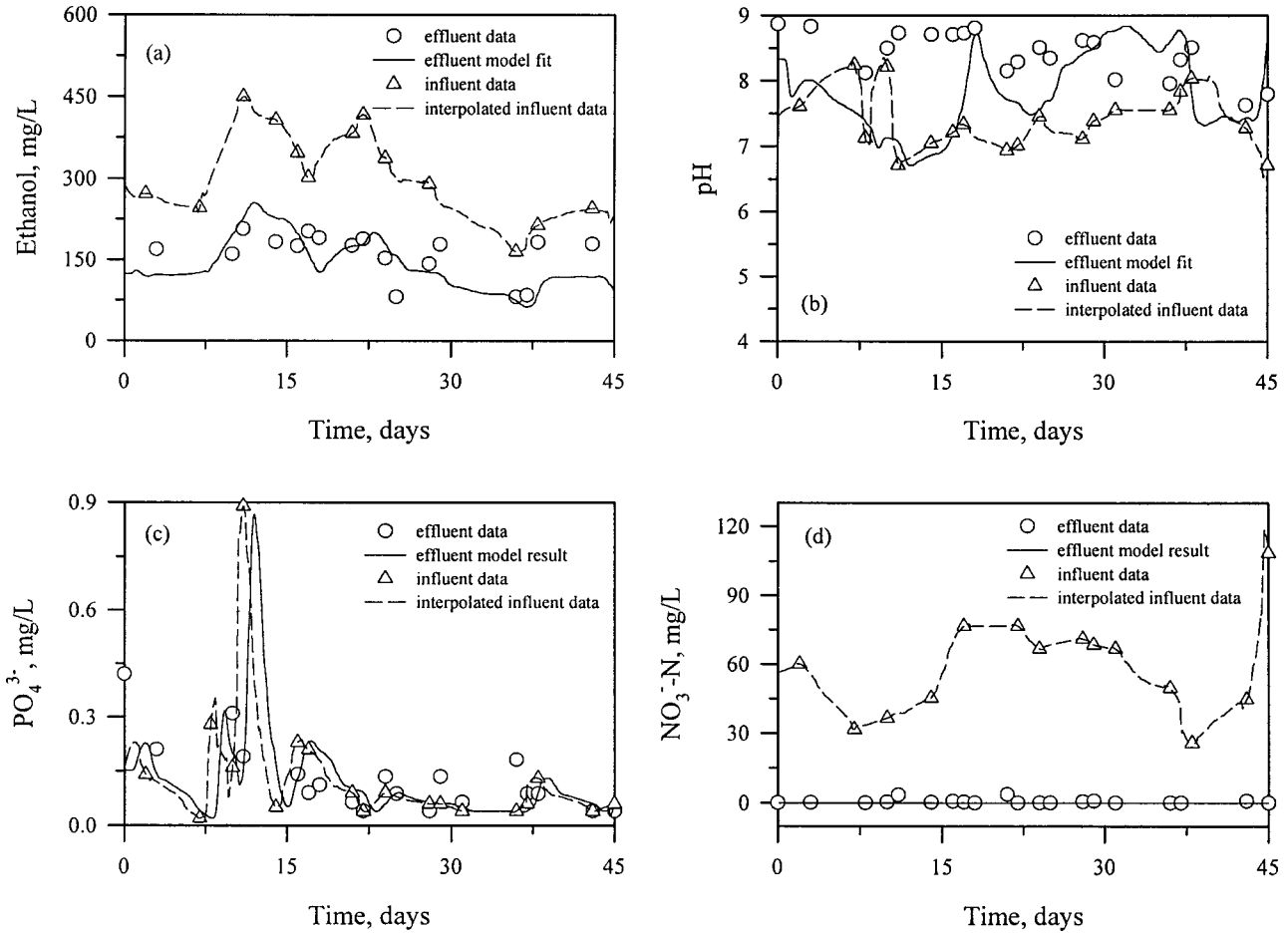

Fig. 6. Experimental data and model fit for (a) ethanol and (b) pH, and experimental data and model results for (c) phosphate and (d) nitrate for biologically active column without the addition of encapsulated buffers but with addition of trichloroethylene (Column A, Case II)

crease the pH to improve the model fit to the pH data, the impact is small because the effluent nitrate levels are already less than 1 mg/L. It would be possible to increase the pH by decreasing $k_{CH_3CH_2OH}$ and hence decreasing CO_2 production. However, this would result in an increase in the ethanol levels and in a higher error that the minimum obtained with Eq. (24). In Case II, difficulties were encountered in controlling the influent pH and nitrate levels to the column. The variability in influent pH is associated with the low feed phosphate levels that resulted in a low influent buffer capacity. Denitrification in the feed tanks, indicated by varying nitrate levels in the influent (most likely due to some biomass growth in the tank and tubing), may have caused an increase in the influent pH.

The difficulties encountered in fitting the model to the data indicate that the model assumptions must be revised to accurately describe the microbiology and solution chemistry of the system and subsequently improve the model fit. Possible revisions to the model include using a biological mechanism different from Eq. (2) that would account for a decrease in the ethanol levels in the system, accounting for cell synthesis and cell decay, and accounting for gas-phase carbon dioxide equilibrium. Although some of these revisions were explored, these were not incorporated in the model because of the lack of appropriate data (e.g., yield coefficients and measurements to verify the second reaction mechanism [i.e., Eq. (2)]).

The kinetic parameters obtained from Column A were used to predict the performance of Column B. Since the primary difference of Column A and Column B was the presence of the encapsulated buffer, it was expected that the pH in Column B would be controlled closer to neutrality when the base neutralization capacity of the microcapsules was not exhausted. The primary assumption in this prediction approach is that the kinetic parameters are not significantly impacted by the pH change in the column. This assumption is based on observations in earlier studies that showed the extent of denitrification to be similar in systems with and without an encapsulated buffer (Vanukuru et al. 1998; Rust et al. 2000; Rust et al. 2002).

Figs. 7 and 8 show the experimental data for Column B for Cases I and II, respectively. Similar to Column A, denitrification was essentially complete in Column B, with an average nitrate removal efficiency of 97 and 99.7% for Cases I and II, respectively. The average ethanol removal efficiency was 69% for Case I, which is essentially the same for Column A. The improvement in ethanol removal efficiency observed for Case II (=73%) compared to Column A, Case II (=52%) could be due to possible microbial phosphate nutrient limitation in Column A. Phosphate nutrient limitations were precluded from Column B because it was added to the column during the release of the encapsulated buffer contents.

The effluent pH from Column B was 8.7 on Day 0 when 5 g of the encapsulated buffer were added to each of the three wells [Case I, see Fig. 7(b)]. The high pH values due by denitrification caused the polymer coating of the encapsulated buffer to dissolve rapidly [see Fig. 2(d) and Fig. 3], releasing the acidic phosphate

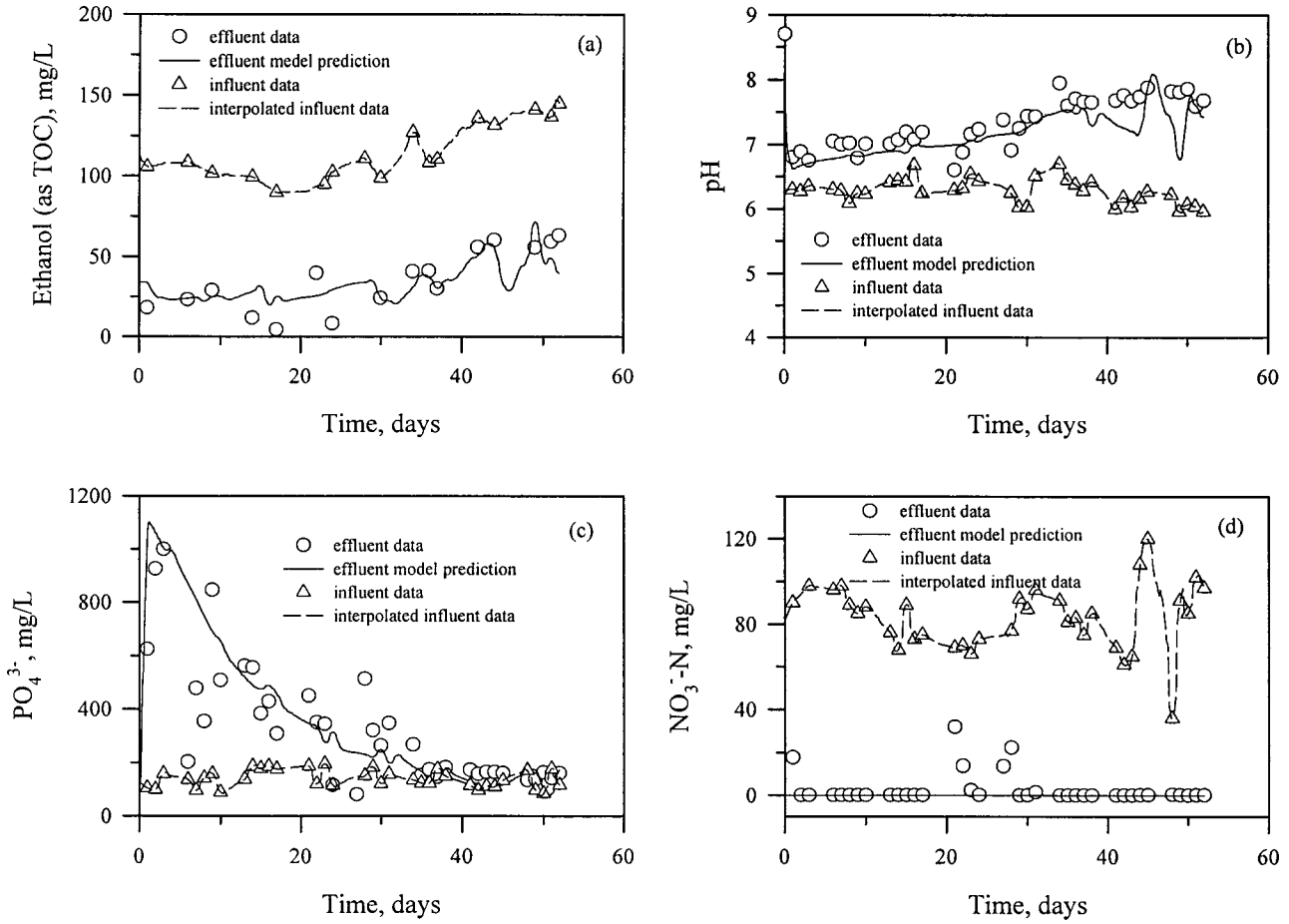

Fig. 7. Experimental data and model predictions for (a) ethanol, (b) pH, (c) phosphate, and (d) nitrate for biologically active column with addition of encapsulated buffers but without addition of trichloroethylene (Column B, Case I)

core into solution. The pH of the effluent dropped to 6.8 1 day after the addition of the encapsulated buffer, and a corresponding rapid increase in the phosphate levels was also observed [see Fig. 7(c)]. A gradual increase in the pH and decrease in phosphate was observed and, after 30 days of operation, the pH was still very close to neutral (=7.4). Similar conclusions may be deduced from the pH and phosphate data of Case II [see Figs. 8(b) and (c)]. The low buffer capacity of the influent feed would lead one to expect that the effluent pH would be higher than the influent pH [as in Fig. 6(b)]. However, the addition of 3 g of encapsulated buffer resulted in the release of the phosphate core and pH levels that are closer to neutrality.

The tendency for an increase in pH due to the continuous denitrification occurring in the column is balanced by a corresponding release in the encapsulated buffer contents to decrease the pH. However, as the encapsulated buffer releases the acidic phosphate core, the base neutralizing capacity of the microcapsules is depleted and eventually exhausted. This is illustrated in Fig. 9 for a theoretical scenario. Without the encapsulated buffer, the pH profiles increase with distance along the column (t =0 days). 10 days after the encapsulated buffer is inserted into the wells, the phosphate level increases and the pH decreases. The points where sudden changes in the profile are observed occur at the microcapsule wells. These profiles change with time as the base neutralizing capacity of the encapsulated buffer is depleted. Ultimately, the profiles are similar to the case where no microcapsules are present.

The model predictions of the performance of Column B are also shown in Figs. 7 and 8. Despite the limitations discussed earlier regarding the model fit to the data for Column A, the model was able to predict the performance of Column B for Case I. Fig. 7 shows that the model correctly predicts the general trends and magnitude of the change in ethanol, pH, phosphate, and nitrate levels in the column effluent with time. However, the model fit to Case II was not as successful. The model correctly predicted the effluent ethanol levels for the first 15 days [see Fig. 8(a)] and the effluent nitrate levels throughout the column run [see Fig. 8(d)]. After 15 days, the model underpredicted the ethanol removal. This discrepancy could be caused by phosphate limitations in Column A, Case II, which would mathematically translate to a low parameter estimate for $k_{CH_3CH_2OH}$. Having a higher value for $k_{CH_3CH_2OH}$ will not change the conclusion that the performance of Column A was not impacted by the presence of TCE.

Although it appears that the initial phosphate rise was overpredicted [see Fig. 8(c)], it is likely that a lack of data in the early days of the column run was not able to capture the sharp initial phosphate peak. After this initial peak, the model was able to correctly predict the decline in phosphate levels with time. Fig. 8(b) shows that the model was able to reasonably predict the effluent pH levels for the initial half of the column run. However, when the base neutralizing capacity of the encapsulated buffer was depleted [as shown by the low effluent phosphate levels in Fig. 8(c) after 22 days], the model predicted an effluent pH that

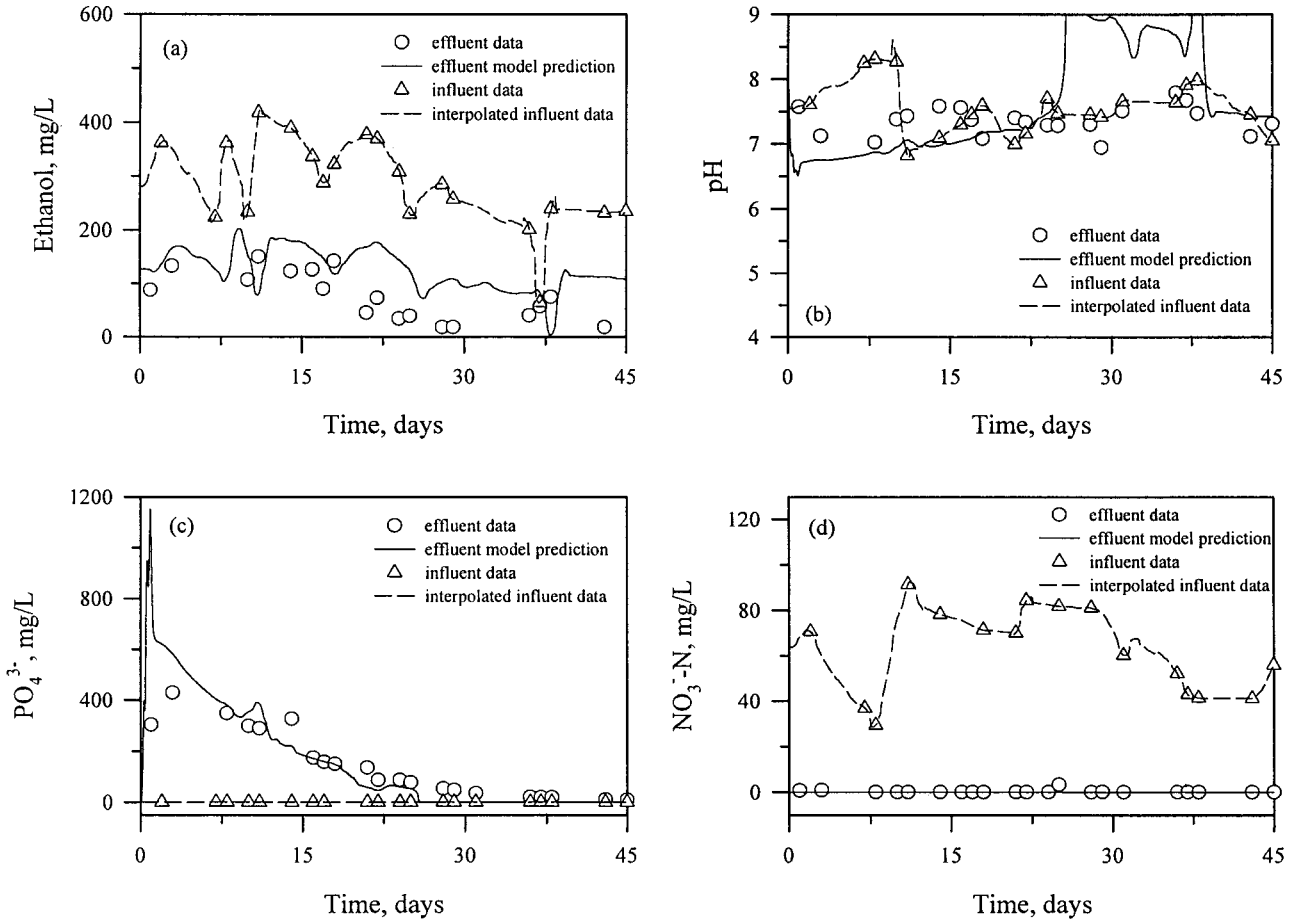

Fig. 8. Experimental data and model predictions for (a) ethanol, (b) pH, (c) phosphate, and (d) nitrate for biologically active column with addition of encapsulated buffers and trichloroethylene (Column B, Case II)

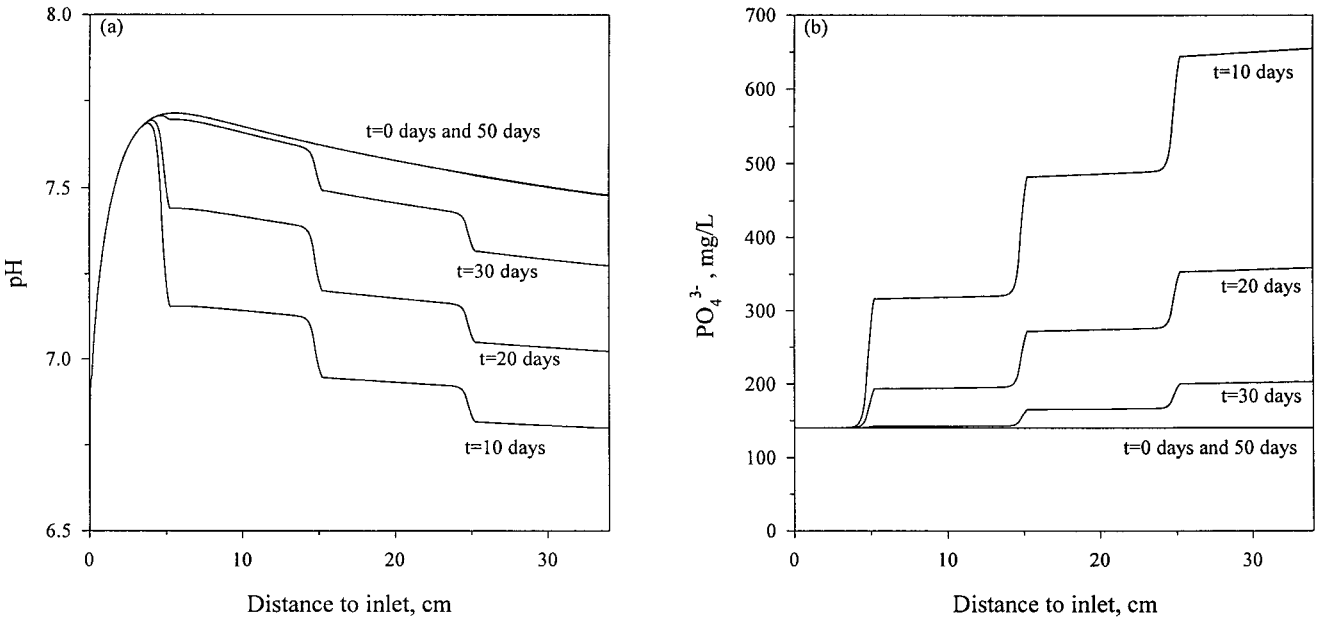

Fig. 9. Theoretical profiles of (a) pH and (b) phosphate along column for constant influent pH of 6.4 and constant influent ethanol, nitrate, carbonate, and phosphate concentrations of 115 mg/L (as total organic carbon), 83, 1.5, and 140 mg/L, respectively, and with 5 g of encapsulated buffer inserted into each well; influent conditions correspond to average influent levels for Fig. 7.

was similar to effluent levels observed in Fig. 6(c). This discrepancy is caused by the model's underestimation of the increase in the rate of ethanol degradation during the latter half of the column run. This rate increase caused the formation of acid equivalents (in the form of carbon dioxide) that resulted in an observed pH drop. The low influent buffer capacity makes pH prediction in the system more sensitive to the assumed biological mechanisms, particularly the amount of carbon dioxide formation. Thus, a more accurate description of the physical system is needed to improve the model predictions.

Conclusions

Denitrification in sand column experiments resulted in an increase in the pH of the effluent from the column. The insertion of encapsulated buffers at three locations along the column resulted in a decrease in the effluent pH through the controlled release of the acidic phosphate buffer core. A one-dimensional model of the sand column was developed that reasonably predicted the release of the encapsulated buffer core and performance of the encapsulated buffer for controlling pH.

Under the conditions and range of pH values that were observed in this study, the rate of denitrification was not sensitive to pH. Thus, the addition of the encapsulated buffer for pH control did not provide a tangible benefit for the system. This does not preclude the utility of the encapsulated buffer because there may be applications where changes in pH may result in less than optimum conditions and may negatively impact the overall goals of the process. For example, researchers have investigated the use of zero-valent metals to induce the in situ remediation of halogenated organic compounds (e.g., Matheson and Tratnyek 1994; Warren et al. 1995; Schlimm and Heitz 1996; Siantar et al. 1996). The corrosion of the metal releases electrons that induce the reduction of the halogenated compound, and the pH rises as the reaction proceeds (Matheson and Tratnyek 1994). This rise in pH is disadvantageous because the kinetics of reduction of the compounds are faster at lower pH values where metal corrosion is enhanced. Thus, it is conceivable that an encapsulated buffer may be used to control the pH to a desirable level.

The effective lifetime of the encapsulated buffer capsule is determined by exposure to high pH conditions [see Figs. 7(c) and 8(c)] and by the diffusion of the contents through the capsule wall at a low pH [see Fig. 2(a)]. Hence, this study shows the effective life of the encapsulated buffer to be limited to several weeks. Thus, for practical application at a full scale, the manufacture of the encapsulated buffer has to be redesigned to release the buffer core contents over at least several months. Once the kinetics of release of the redesigned encapsulated buffer and the site conditions are characterized, the modeling approach illustrated in this paper can be used to evaluate the theoretical effectiveness of the encapsulated buffer in controlling the pH. Most importantly, because implementation of the technology would require the introduction of the encapsulated buffer as a point source, the modeling approach should be expanded to at least two dimensions to evaluate the region of effectiveness of the capsule and design the points of encapsulated buffer injection.

Acknowledgments

This material is based upon work supported in part by Grant No. DE-FGO2-97EW09999 from the U.S. Department of Energy, Office of Environmental Management to the Center for Water Research and Policy and the National Science Foundation (Flora, Grant No. BES-9733377). Any opinions, findings, and conclusions or recommendations expressed in this manuscript are those of the writers and do not necessarily reflect the views of the funding agency. Mention of any specific trade name does not constitute endorsement of the product by the writers or the sponsors.

Notation

The following symbols are used in this paper:

C_j = concentration of species j;
$C_{j,\text{inf}}$ = influent concentration of species j;
$C_{j,0}$ = initial concentration of species j;
$C_{T,j}$ = total concentration of species j;
D = dispersion coefficient;
$[j]$ = molar concentration of species j;
$K_{i,j}$ = jth dissociation constant of ith species;
K_w = equilibrium constant of water dissociation;
k_j = first-order reaction rate constant for species j;
L = length of sand column;
M_c = mass of encapsulated buffer core;
MW_j = molecular weight of species j;
Q = flow rate in column;
R = radius of sand column;
R_i = rate of production of species i;
$R_{i,j}$ = rate of production of species i for reaction j;
SSE = sum of squares of errors;
t = time;
u = linear water velocity through column $= Q/\varepsilon\pi R^2$;
V_{well} = volume of well;
x = axial distance along column;
α = first order kinetic constant for release rate of encapsulated buffer core; and
ε = porosity of sand column.

References

Albrechtsen, H.-J. (1994). "Bacterial degradation under iron reducing conditions." *Hydrocarbon bioremediation*, R. E. Hinchee, B. C. Alleman, R. E. Hoeppel, and R. N. Miller, eds., Lewis, Boca Raton, Fla., 418–423.

Allison, J. D., Brown, D. S., and Novo-Gradac, K. J. (1991). "MINTEQA2/PRODEFA2, A geochemical assessment model for environmental system." *EPA/600/3-91/021*, U.S. Environmental Protection Agency, Cincinnati.

Appelo, C. A. J. (1994). "Cation and proton exchange, pH variations, and carbonate reactions in a freshening aquifer." *Water Resour. Res.*, 30(10), 2793–2805.

Bäverman, C., Strömberg, B., Moreno, L., and Neretnieks, I. (1999). "CHEMFRONTS: A coupled geochemical and transport simulation tool." *J. Contam. Hydrol.*, 36(3–4), 333–351.

Choi, J., Hulseapple, S. M., Conklin, M. H., and Harvey, J. W. (1998). "Modeling CO_2 degassing and pH in a stream-aquifer system." *J. Hydrol.*, 209, 297–310.

Furrer, G., von Gunten, U., and Zobrist, J. (1996). "Steady-state modelling of biogeochemical processes in columns with aquifer material: 1. Speciation and mass balances." *Chem. Geol.*, 133, 15–28.

Goodwin, S., Conrad, R., and Zeikus, J. G. (1988). "Influence of pH on microbial hydrogen metabolism in diverse sedimentary ecosystems."

Appl. Environ. Microbiol., 54, 590–593.
Haran, B. S., Popov, B. N., Zheng, G., and White, R. E. (1997). ''Mathematical modeling of hexavalent chromium decontamination from low surface charged soils.'' *J. Haz. Mat.*, 55, 93–107.
Levenspeil, O. (1993). *The chemical reactor omnibook*, OSU Book Stores, Corvallis, Ore.
Matheson, L. J., and Tratnyek, P. G. (1994). ''Reductive dehalogenation of chlorinated methanes by iron metal.'' *Environ. Sci. Technol.*, 28, 2045–2053.
Neter, J., Wasserman, W., and Kutner, M. H. (1990). *Applied linear statistical models*, 3rd Ed., Richard C. Irwin, Inc., Homewood, Ill.
Parkhurst, D. L. (1995). *User's guide to PHREEQC—A computer program for speciation, reaction-path, advective-transport, and inverse geochemical calculations*, U.S. Geological Survey, Lakewood, Colo.
Patankar, S. V. (1980). *Numerical heat transfer and fluid flow*, McGraw-Hill, New York.
Reardon, K. F., and Bailey, J. E. (1989). ''Effects of pH and added metabolites on bioconversions by immobilized non-growing *Clostridium acetobutylium*.'' *Biotechnol. Bioeng.*, 34, 825–837.
Rust, C. M. (2001). ''Enhancing microbial trichloroethylene dechlorination by controlling pH with encapsulated phosphate buffer.'' PhD thesis, Univ. of South Carolina, Columbia, S.C.
Rust, C. M., Aelion, C. M., and Flora, J. R. V. (2000). ''Control of pH during denitrification in subsurface sediment using encapsulated phosphate buffer.'' *Water Res.*, 34(5), 1447–1454.
Rust, C. M., Aelion, C. M., and Flora, J. R. V. (2002). ''Laboratory sand column study of encapsulated buffer release for potential in situ pH control.'' *J. Contam. Hydrol.*, 54(1–2), 81–98.
Schlimm, C., and Heitz, E. (1996). ''Development of a wastewater treatment process: Reductive dehalogenation of chlorinated hydrocarbons by metals.'' *Environ. Prog.*, 15, 38–47.
Siantar, D. P., Schreier, C. G., Chou, C.-S., and Reinhard, M. (1996). ''Treatment of 1,2-dibromo-3-chloropropane and nitrate-contaminated water with zero-valent iron or hydrogen/palladium catalysts.'' *Water Res.*, 30, 2315–2322.
Snoeyink, V. L., and Jenkins, D. (1980). *Water chemistry*, Wiley, New York.
Vanukuru, B., Flora, J. R. V., Petrou, M. F., and Aelion, C. M. (1998). ''Control of pH during denitrification using an encapsulated phosphate buffer.'' *Water Res.*, 32(9), 2735–2745.
von Gunten, U., and Furrer, G. (2000). ''Steady-state modeling of biogeochemical processes in columns with aquifer material: 2. Dynamics of iron-sulfur interactions.'' *Chem. Geol.*, 167, 271–284.
Warren, K. D., Arnold, R. G., Bishop, T. L., Lindholm, L. C., and Betterton, E. A. (1995). ''Kinetics and mechanism of reductive dehalogenation of carbon tetrachloride using zero-valence metals.'' *J. Haz. Mat.*, 41, 217–227.
Wolery, T. J. and Daveler, S. A. (1992). ''*EQ6*. A computer program for reaction path modeling of aqueous geochemical system.'' *Theoretical manual, user's guide, and related documentation (Version 7.0)*, Lawrence Livermore National Laboratory, Livermore, Calif.